Interlayer and interfacial exchange coupling in ferromagnetic metal/semiconductor heterostructures

M. J. Wilson,[1] M. Zhu,[1] R. C. Myers,[2] D. D. Awschalom,[2] P. Schiffer,[1] and N. Samarth[1,*]
[1]*Department of Physics, The Pennsylvania State University, University Park, Pennsylvania 16802, USA*
[2]*Department of Physics, University of California, Santa Barbara, California 93106, USA*
(Received 21 May 2009; revised manuscript received 16 December 2009; published 25 January 2010)

We describe a systematic study of the exchange coupling between a magnetically hard metallic ferromagnet (MnAs) and a magnetically soft ferromagnetic semiconductor ($Ga_{1-x}Mn_xAs$) in bilayer and trilayer heterostructures. An exchange spring model of $MnAs/Ga_{1-x}Mn_xAs$ bilayers accounts for the variation in the exchange-bias field with layer thickness and composition. We also present evidence for hole-mediated interlayer exchange coupling in $MnAs/p$-$GaAs/Ga_{1-x}Mn_xAs$ trilayers and study the dependence of the exchange-bias field on the thickness of the spacer layer.

DOI: 10.1103/PhysRevB.81.045319 PACS number(s): 75.50.Pp, 75.75.−c, 81.16.−c

I. INTRODUCTION

The systematic study of interlayer and interfacial exchange coupling in ferromagnetic (FM) metal multilayers has led to important advances in condensed-matter physics, in addition to guiding rapid progress in magnetic storage technologies.[1,2] In a similar manner, fundamental inquiry into the exchange coupling in FM semiconductor heterostructures could have an important influence on the development of semiconductor spintronics, where one can envision an additional level of optoelectronic control over the underlying exchange interaction.[3] Interlayer and/or interfacial exchange coupling in FM semiconductor heterostructures has indeed been unequivocally observed in a variety of experiments, including neutron-scattering measurements of $Ga_{1-x}Mn_xAs/GaAs$ multilayers,[4,5] magnetometry, and magnetoresistance measurements of $MnO/Ga_{1-x}Mn_xAs$ bilayers[6,7] and $MnAs/Ga_{1-x}Mn_xAs$ bilayers,[8] and x-ray magnetic circular dichroism studies of $Fe/Ga_{1-x}Mn_xAs$ heterostructures.[9] However, despite long-standing theoretical interest in this topic,[10] there is little systematic experimental data that examines the dependence of this coupling on relevant parameters; the availability of such data is critical for developing a deeper theoretical understanding of interfacial/interlayer exchange coupling in FM semiconductor heterostructures.

This paper presents systematic studies of the interlayer and interfacial exchange coupling between a magnetically soft FM semiconductor ($Ga_{1-x}Mn_xAs$) and a magnetically hard FM metal (MnAs). The juxtaposition of these materials is particularly convenient because the interlayer and interfacial exchange coupling are readily measured using standard magnetometry techniques,[8] rather than requiring more elaborate methods such as neutron scattering[4,5] or x-ray magnetic circular dichroism (XMCD).[9] We systematically map out the variation in the exchange coupling as a function of many sample parameters in both bilayer and trilayer geometries. Our group has previously examined exchange coupling in bilayers as a function of $Ga_{1-x}Mn_xAs$ thickness (t_{GMA}), showing that the exchange field (H_E) varies inversely with t_{GMA}.[8] The present work first confirms this result in an additional set of samples and then goes on to study the dependence of the exchange coupling on a wide range of previously unexplored parameters such as MnAs thickness, magnetization, and spacer thickness in trilayer systems, all of which give important insights into the physics of this system. The results are consistent with the formation of an exchange spring in bilayers due to FM interfacial coupling with MnAs.[11] Additionally, in trilayers, we find evidence for FM hole-mediated exchange coupling that decays exponentially with spacer-layer thickness, persisting over a length scale of ~5 nm. We do not find evidence for antiferromagnetic (AFM) exchange coupling over the entire space of parameters examined. This is in contrast to the reported observation of AFM interlayer coupling in neutron-scattering studies of a $Ga_{1-x}Mn_xAs/p$-$GaAs/Ga_{1-x}Mn_xAs$ multilayer sample.[5] Finally, we find an enhancement of the Curie temperature (T_C) of $Ga_{1-x}Mn_xAs$ layers by the overgrowth of MnAs. Although superficially resembling a "proximity effect" wherein the T_C of a weak ferromagnet might be enhanced by interfacial exchange coupling with a strong ferromagnet,[9] control measurements show that this is an extrinsic effect stemming from the unintentional annealing during growth.

II. EXPERIMENTAL DETAILS

This paper focuses on four different series of samples. Series A consists of three bilayer samples with 12 nm "type-A" MnAs on top of a $Ga_{1-x}Mn_xAs$ layer with $x \sim 6\%$ and with $Ga_{1-x}Mn_xAs$ layer thicknesses of $t_{GMA}=30$, 50, and 80 nm. Series B consists of three $MnAs/Ga_{1-x}Mn_xAs$ bilayers where the composition of the $Ga_{1-x}Mn_xAs$ is varied ($0.05 \leq x \leq 0.16$) while keeping the $Ga_{1-x}Mn_xAs$ and MnAs thicknesses constant at 30 and 8 nm, respectively. Series C consists of several $MnAs/Ga_{1-x}Mn_xAs$ bilayer samples ($x \sim 6\%$, $t_{GMA}=30$ nm) in which the MnAs layer is purposely varied in thickness ($1 \lesssim t_{MA} \lesssim 4$ nm) across the wafer by exposing the static substrate to a spatially inhomogeneous Mn flux. Series D consists of $MnAs/p$-$GaAs/Ga_{1-x}Mn_xAs$ trilayers (with $x \sim 6\%$) in which the MnAs and $Ga_{1-x}Mn_xAs$ layer thicknesses are kept fixed ($t_{MA}=10$ nm and $t_{GMA}=30$ nm) while the spacer thickness is varied ($t_{spacer}=1,2,3,4,5$ nm).

The heterostructures used in our studies are fabricated by low-temperature molecular-beam epitaxy on semi-insulating

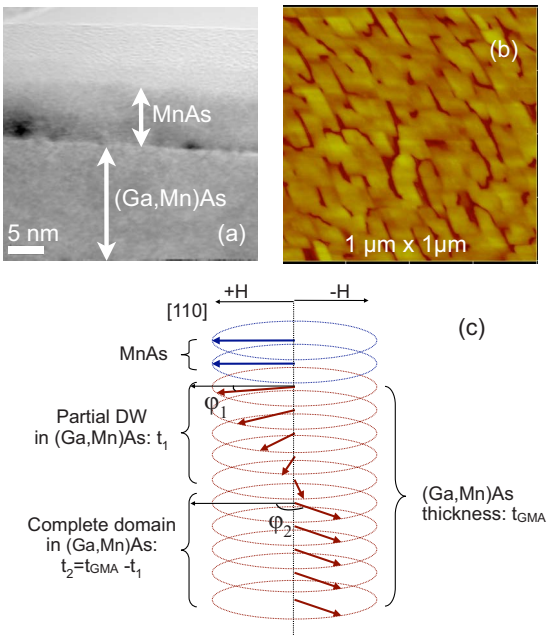

FIG. 1. (Color online) (a) High-resolution TEM images of a bilayer sample. (b) Atomic force microscope image of the top MnAs layer. (c) Depiction of a partial domain-wall configuration in $Ga_{1-x}Mn_xAs$, with spins continuously rotating as a function of the distance from the interface. Beyond a certain depth t_1, a complete domain (t_2) forms.

(001) GaAs substrates, after first depositing a 170-nm-thick high-temperature grown GaAs buffer layer at 580 °C. This is followed by the growth of a $Ga_{1-x}Mn_xAs$ layer at a substrate temperature in the range 235–250 °C; the optimal substrate temperature depends on the Mn concentration. In particular, we note the use of distinct conditions during the growth of the highest Mn composition bilayer sample used in series B.[12] For trilayer samples, the epitaxial growth proceeds with deposition of a *p*-doped GaAs:Be layer at the same substrate temperature. The carrier concentration is approximately 3×10^{19} cm^{-3} as determined by Hall-effect measurements of control samples. After the growth of the $Ga_{1-x}Mn_xAs$ layer (or $Ga_{1-x}Mn_xAs/p$-GaAs heterostructure), the substrate temperature is lowered to ~200 °C with the As shutter open to initiate the growth of a few monolayers of MnAs under As-rich conditions. The substrate temperature is then raised to ~230 °C and MnAs growth is resumed; this procedure consistently yields MnAs in the type-A orientation with the *c* axis aligned with the $[\bar{1}10]$ axis of the $Ga_{1-x}Mn_xAs$ layer.

Cross-sectional transmission electron microscopy (TEM) shows an atomically abrupt and smooth interface between MnAs and $Ga_{1-x}Mn_xAs$, despite a large lattice mismatch [Fig. 1(a)]. Atomic force microscopy measurements show that the freshly grown MnAs surface exhibits a relatively smooth surface with an rms roughness of about 1 nm [Fig. 1(b)]. Some trenches with depth of ~2 nm are observed as a result of the transition from three-dimensional island growth to two-dimensional layer growth. Note that the MnAs layer oxidizes quite readily, thus necessitating sample storage in vacuum for observing consistent physical properties with aging. The magnetic properties of the samples are characterized using a dc superconducting quantum interference device (SQUID) magnetometer. For temperature-dependent measurements of the magnetization $M(T)$, samples are first cooled down from room temperature in a 20 kOe field applied along the easy axis of MnAs; unless otherwise stated, measurements are then taken while warming up in a field of 30 Oe. For magnetization hysteresis measurements, we focus here only on minor loops of the $Ga_{1-x}Mn_xAs$ layers in order to determine the exchange field. The minor loops are taken to a positive field large enough to switch the $Ga_{1-x}Mn_xAs$ layer (typically 500–1200 Oe) but smaller than the coercivity of MnAs, which is around 2 kOe. The hysteresis loops are measured after first saturating the MnAs layer in a negative 20 kOe field. All hysteresis loops unless noted are measured at 4.2 K and the applied field is along the [110] GaAs crystalline axis. This corresponds to the $[11\bar{2}0]$ direction in MnAs, which is the easy axis of the type-A MnAs layer.

III. EXCHANGE SPRING MODEL OF BILAYERS

We begin by discussing the interfacial exchange coupling in $MnAs/Ga_{1-x}Mn_xAs$ bilayers. To calculate the exchange field experienced by the $Ga_{1-x}Mn_xAs$ layer, we use a partial domain wall (PDW) model analogous to the one used in AFM/FM systems[13] and hard/soft metallic FM bilayers.[14] The magnetization of MnAs is considered to be fixed along its easy axis in the positive field direction along the [110] axis of $Ga_{1-x}Mn_xAs$; this corresponds to the $[11\bar{2}0]$ direction of the hexagonal MnAs crystal. The magnetization of the $Ga_{1-x}Mn_xAs$ layer is free to switch in an external magnetic field and its direction is designated with reference to the fixed MnAs magnetization, as illustrated in Fig. 1(c). We assume that a PDW of thickness t_1 is formed in the $Ga_{1-x}Mn_xAs$ layer near the interface. The angle between the MnAs magnetization and the $Ga_{1-x}Mn_xAs$ magnetization at the interface is defined as φ_1 while φ_2 is the angle between the MnAs magnetization and the bulk $Ga_{1-x}Mn_xAs$ magnetization. Due to the strong coupling at the interface and the relatively strong anisotropy constant of MnAs, the interfacial spin alignment of the $Ga_{1-x}Mn_xAs$ layer should be very close to that in the MnAs layer. For this strong interfacial coupling, where $\varphi_1 \approx 0$ and $t_1 \ll t_2 \approx t_{GMA}$, the energy density per unit area can be written as

$$E = 2\sqrt{AK}(1-\cos\varphi_2) - A_{ex} + K_u t_{GMA}\sin^2\varphi_2 + 1/4K_c t_{GMA}\cos^2 2\varphi_2 - HMt_{GMA}\cos\varphi_2. \quad (1)$$

The first term is the energy of the PDW, where A is the spin stiffness of $Ga_{1-x}Mn_xAs$ and K is the effective anisotropy constant; the second term (A_{ex}) is the exchange coupling at the interface; the third and fourth terms are the uniaxial and biaxial anisotropy energy in $Ga_{1-x}Mn_xAs$. The terms K_u and K_c are the uniaxial and biaxial anisotropy constants, respectively. The last term is the Zeeman energy where H is the externally applied magnetic field and M is the saturated magnetization of the $Ga_{1-x}Mn_xAs$ layer. When considering a strong cubic anisotropy, the energy minimum occurs at 45° and 135°. Thus, the two switching fields are determined by using the following two conditions:

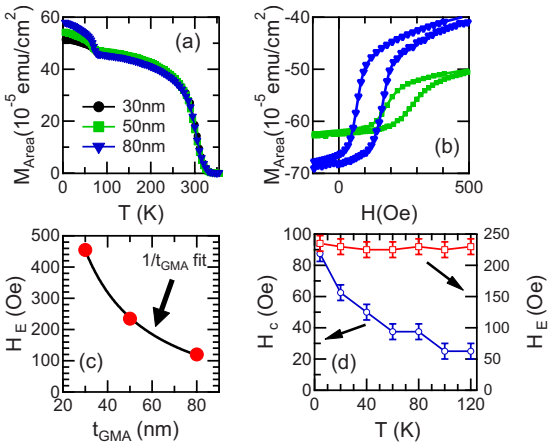

FIG. 2. (Color online) (a) Temperature-dependent remanent magnetization $M(T)$ for bilayer samples with three different $Ga_{1-x}Mn_xAs$ thicknesses as indicated on the plot (series A). The $Ga_{1-x}Mn_xAs$ composition is $x=0.06$ and the MnAs thickness is $t_{MA}=12$ nm. (b) Minor hysteresis loop for the bilayer samples with $t_{GMA}=50$ nm (green squares) and $t_{GMA}=80$ nm (blue triangles). Data are taken at $T=4.2$ K. (c) Exchange field versus $Ga_{1-x}Mn_xAs$ thickness, showing that $H_E \propto (t_{GMA})^{-1}$. Data are taken at $T=4.2$ K. (d) Coercivity and exchange field as a function of temperature for a high Mn composition $MnAs/Ga_{1-x}Mn_xAs$ bilayer with $t_{GMA}=50$ nm and $x=0.16$.

$\frac{\partial^2 E}{\partial \varphi_2^2}(\varphi_2=\pi/4)>0$, $\frac{\partial^2 E}{\partial \varphi_2^2}(\varphi_2=3\pi/4)>0$. This yields the following switching fields:

$$H > H_{C1} = \frac{-2\sqrt{2AK} - 4K_c t}{\sqrt{2}Mt}, \tag{2}$$

$$H > H_{C2} = \frac{-2\sqrt{2AK} + 4K_c t}{\sqrt{2}Mt}. \tag{3}$$

The exchange field, given by $H_E=(H_{C1}+H_{C2})/2=-2\sqrt{AK}/Mt$, shows an inverse dependence on both the thickness and magnetization of the $Ga_{1-x}Mn_xAs$ layer. In addition, the model also predicts that the coercive field, given by $H_c=(H_{C2}-H_{C1})=8K_c/\sqrt{2}M$, shows an inverse dependence on the magnetization of the $Ga_{1-x}Mn_xAs$ layer. The validity of this model is tested by studying the exchange coupling in $MnAs/Ga_{1-x}Mn_xAs$ bilayers as a function of sample geometry and composition.

IV. VARIATION IN EXCHANGE FIELD AND COERCIVE FIELD WITH $Ga_{1-x}Mn_xAs$ THICKNESS IN BILAYERS

We first address the effect of varying the $Ga_{1-x}Mn_xAs$ layer thickness (series A). Figure 2(a) shows the temperature dependence of the remanent magnetization $M(T)$ in three bilayer samples with $t_{GMA}=30$, 50, and 80 nm, measured in a field of 30 Oe after cooling down from room temperature in a −20 kOe field. Note that the plot depicts the magnetization of the films normalized to area (not volume) since the samples are bilayer stacks of two different ferromagnets. We clearly observe two distinct FM phase transitions at $T_C \sim 75$ K for $Ga_{1-x}Mn_xAs$ and $T_C \sim 318$ K for MnAs. The major magnetization hysteresis loops (data not shown) are similar to the data shown on other samples in a previous report,[8] revealing two different coercivities for $Ga_{1-x}Mn_xAs$ (~100 Oe) and MnAs (~2 kOe). Based upon our SQUID measurements of these major hysteresis loops, we do not find any obvious indications of a biquadratic coupling. Figure 2(b) shows the minor loops for two bilayers with different $Ga_{1-x}Mn_xAs$ thicknesses; the displacement of the center of the minor loop is always opposite to the magnetization of the MnAs layer, indicating a "negative exchange bias" due to FM coupling between the two layers, where a parallel alignment of the two layers is favored. Note that this FM coupling contrasts with the AFM coupling reported in XMCD studies of $Fe/Ga_{1-x}Mn_xAs$ bilayers.[9] The opposite sign of the interfacial exchange coupling in $MnAs/Ga_{1-x}Mn_xAs$ and $Fe/Ga_{1-x}Mn_xAs$ is very intriguing but we do not presently have an explanation for this difference in behavior. We find that the exchange field $H_E \sim (t_{GMA})^{-1}$, in agreement with our model [Fig. 2(c)] and consistent with earlier measurements on a different sample series.[8] With typical parameters for $Ga_{1-x}Mn_xAs$ samples of comparable composition ($A \sim 0.4$ pJ/m, $K \sim 0.3$ kJ/m^3, and $M \sim 16\,000$ A/m^3),[15] we calculate $H_E \sim 440$, 264, and 165 Oe for the bilayers with $t_{GMA}=30$, 50, and 80 nm, respectively. This agrees reasonably well with the respective experimental values of 455, 235, and 120 Oe. The PDW model also predicts that the coercive field H_c should be independent of t_{GMA}; our data are in agreement with this, with no obvious experimental dependence found in all three samples in Fig. 2(c).

Studies of ferromagnets exchange biased by an antiferromagnet typically show a correlation between H_E and the coercive field H_c. This relationship can be studied by examining the temperature dependence of H_E and H_c. For this purpose, we chose a $MnAs/Ga_{1-x}Mn_xAs$ bilayer with high Mn concentration ($x=0.16$) since this leads to a higher T_C ($=160\pm5$ K),[12] thus allowing us to cover a wider temperature range. In contrast to conventional exchange biasing using an antiferromagnet, we find that the H_c and H_E are not correlated while H_c decreases with increasing temperature, H_E stays relatively constant [Fig. 2(d)]. The decrease in coercivity is expected and is also seen in nonexchange-biased $Ga_{1-x}Mn_xAs$ samples where it is attributed to a weakening of the magnetization and anisotropies of the $Ga_{1-x}Mn_xAs$ layer. However, the constant exchange field is surprising; the PDW model predicts that as the magnetization of the $Ga_{1-x}Mn_xAs$ layer decreases with increasing temperature, H_E should increase. However, we note that the anisotropy constants of $Ga_{1-x}Mn_xAs$ are also a function of temperature, decreasing with increasing temperature.[15,16] Thus, a possible reason for our observation is that the temperature dependence of both the magnetization and anisotropy cancel out any temperature variation in H_E.

V. VARIATION IN EXCHANGE FIELD AND COERCIVE FIELD WITH $Ga_{1-x}Mn_xAs$ MAGNETIZATION IN BILAYERS

A second prediction of the model is that H_E should decrease inversely with the saturated magnetization (M_{sat}) of

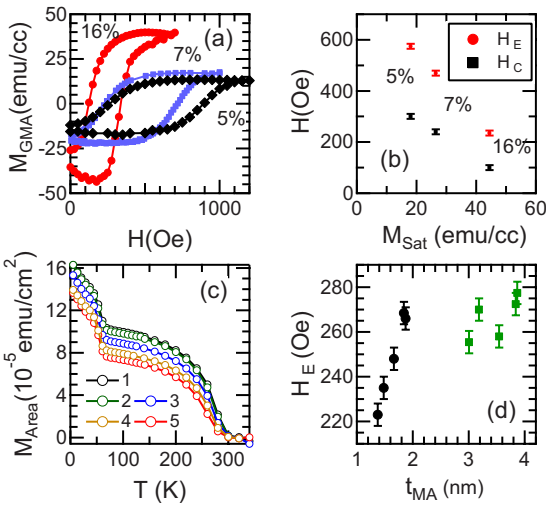

FIG. 3. (Color online) (a) Minor hysteresis loops of three bilayer samples with varying composition $x=0.05, 0.07, 0.16$ (series B). In these three samples, $t_{GMA}=30$ nm and $t_{MA}=8$ nm. The magnetization is shown per unit volume with the MnAs signal subtracted out. Data are taken at $T=4.2$ K. (b) Exchange field (H_E) and coercivity (H_c) as a function of the saturated magnetization. Data are taken at $T=4.2$ K. (c) Temperature-dependent remanent magnetization $M(T)$ for bilayer samples with different MnAs layer thicknesses in the range $1 \lesssim t_{MA} \lesssim 4$ nm (series C). The $Ga_{1-x}Mn_xAs$ layer has a thickness $t_{GMA}=30$ nm and composition $x=0.06$. The magnetization is shown per unit area. (d) Exchange field versus MnAs layer thickness showing critical thickness between 2 and 3 nm. The different symbols refer to two different nonrotated growths. Data are taken at $T=4.2$ K.

the $Ga_{1-x}Mn_xAs$ layer. This prediction is tested with a series of samples of varied Mn content (Series B). Figure 3(a) shows the minor loops of three samples with varying saturation of $Ga_{1-x}Mn_xAs$ layer with nominal values of $x \approx 0.05, 0.07, 0.16$. Figure 3(b) shows that the data are qualitatively consistent with the model (i.e., H_E decreases with increasing M_{sat}) but deviate from the predicted inverse dependence. A plausible explanation for this deviation is that the changing Mn composition will also change the anisotropy constants and not just saturated magnetization. Also shown in Fig. 3(b) is the coercivity as a function of magnetization, which is qualitatively consistent with the $(M_{sat})^{-1}$ dependence predicted by the model.

VI. VARIATION IN EXCHANGE FIELD WITH MnAs THICKNESS IN BILAYERS

In the PDW model, the MnAs layer is treated as being essentially infinitely thick. In order to investigate the limitations of this assumption, we now address the behavior of bilayer samples in which the thickness of the MnAs layer (t_{MA}) is varied, keeping t_{GMA} fixed (series C). These samples were grown by stopping the rotation of the wafer during the growth of the MnAs layer, allowing for a spatial variation in MnAs thickness across a single wafer. We grew two wafers and cut each into five separate samples. Figure 3(c) shows $M(T)$ for the first set of samples with $1.4 \lesssim t_{MA} \lesssim 2$ nm, where we estimate t_{MA} using the saturated magnetization. The second set has estimated values $3 \lesssim t_{MA} \lesssim 4$ nm. Note that all these thicknesses are significantly thinner than our other sets of samples, which had $t_{MA} \gtrsim 8$ nm. Figure 3(d) shows H_E vs t_{MA} for both sets of samples (differentiated by the color of the data points); the plot indicates that H_E shows little dependence on t_{MA} for bilayer samples with at least 3 nm of MnAs, which is consistent with the PDW model. However, Fig. 3(d) also shows that H_E rapidly decreases for very thin layers of MnAs ($t_{MA} \lesssim 2$ nm).

The observed variation in the exchange field on the thickness of the biasing MnAs layer is reminiscent of the behavior in the conventional exchange-biasing effect provided by an antiferromagnet.[17] Using the simple Meiklejohn-Bean model, exchange biasing is obtained under the condition $K_{AFM}t_{AFM} \gg A_{ex}$, where K_{AFM} and t_{AFM} are the anisotropy and the thickness of the AFM layer and A_{ex} is the interfacial exchange coupling. This model (and its more sophisticated extensions) thus predict that a critical thickness of the AFM layer is needed for exchange biasing with a value proportional to the ratio $\frac{A_{ex}}{K_{AFM}}$. Studies of AFM/FM bilayers have confirmed in some detail the expectations of this picture, showing both the quenching of exchange bias below a critical value as well as a saturation of the exchange bias at large AFM layer thickness.[18] It is tempting to state that a similar picture could explain the variation in the exchange field with the MnAs layer thickness; the only difference between our hard/soft FM bilayers and conventional AFM/FM bilayers is that the term describing the energy of the biasing layer depends upon the anisotropy of a ferromagnet rather than an antiferromagnet. Thus, our observation of an exchange field that saturates for rather small values of the biasing layer thickness ($t_{MA} \gtrsim 2$ nm) could be viewed as being qualitatively consistent with the relatively large anisotropy of the MnAs layer compared with the interfacial exchange-coupling energy.

VII. INTERLAYER EXCHANGE COUPLING IN $Ga_{1-x}Mn_xAs$/GaAs/MnAs TRILAYERS: VARIATION WITH THICKNESS AND DOPING OF SPACER LAYER

Next, we address the propagation of the exchange coupling through a nonmagnetic spacer by studying the behavior of MnAs/p-GaAs/$Ga_{1-x}Mn_xAs$ trilayers (series D). Our data provide evidence that the exchange coupling between the two FM layers is mediated by holes in the spacer. Figure 4(a) shows a comparison between minor hysteresis loops for two samples with a 3 nm spacer, one of which is *undoped* and the other doped with a nominal hole concentration of 3×10^{19} cm^{-3}. There is no evidence for exchange biasing in the sample with the undoped spacer while the doped sample shows a clear shift, thus strongly suggesting that the exchange between the two magnetic layers is hole mediated. A systematic study of this coupling as a function of the doping density is beyond the scope of this paper. Instead, we focus on the spacer thickness (t_{spacer}) for a fixed p-doping level in the spacer. Figure 4(b) shows both H_E and H_c as a function of t_{spacer}, indicating that the exchange coupling becomes

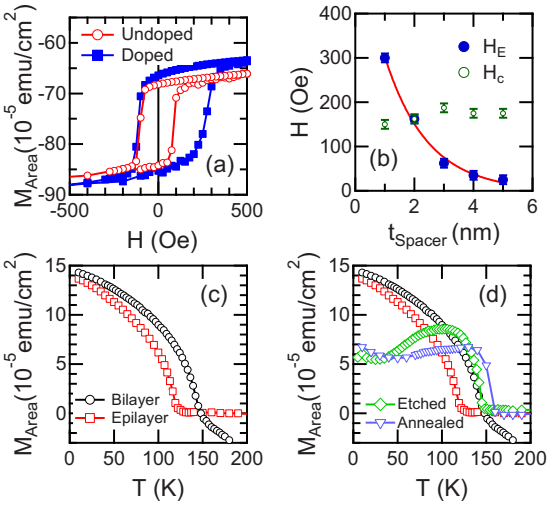

FIG. 4. (Color online) (a) Minor loops for two trilayer samples, one with an undoped spacer and one with a Be-doped spacer. Data are taken at T=4.2 K. The $Ga_{1-x}Mn_xAs$, MnAs, and spacer-layer thicknesses are t_{GMA}=30 nm, t_{MA}=12 nm and t_{spacer}=3 nm, respectively. (b) Exchange field (H_E) and coercivity (H_c) in $Ga_{1-x}Mn_xAs/p$-GaAs/MnAs trilayers versus p-GaAs spacer-layer thickness (series D). Here, t_{GMA}=30 nm and t_{MA}=10 nm. Data are taken at T=4.2 K. The solid line shows a fit of the variation in H_E vs t_{spacer} to an exponential decay: $H_E \propto \exp(-\alpha t_{spacer})$. (c) Temperature-dependent magnetization $M(T)$ for bilayer and single-layer control sample. These measurements are taken while warming up in a field of 200 Oe. (d) Same as in (c) with the added etched sample showing that T_C did not change and with added annealed control sample showing very similar increase in T_C. The unusual shape of the $M(T)$ at lower temperatures results from temperature-dependent changes in the easy axis.

negligible when the spacer is larger than 5 nm (around the anticipated spin-diffusion length in Be-doped GaAs). The plot also shows that H_E decays exponentially with t_{spacer} [as indicated by the fit in Fig. 4(b)] while H_c is relatively constant. The robustness of this behavior has been confirmed in a second set of trilayer samples (not shown). Note there is no evidence for AFM exchange coupling over the entire space of parameters examined; this differs from the findings of a recent neutron-scattering study of a $Ga_{1-x}Mn_xAs/p$-GaAs/$Ga_{1-x}Mn_xAs$ superlattice sample that revealed hole-mediated AFM coupling between the $Ga_{1-x}Mn_xAs$ layers.[5] We speculate that this difference probably arises from the very different electronic structure and densities of states in these two systems; our studies probe the exchange coupling between a metallic FM and a FM semiconductor while the neutron-scattering measurements center around the exchange coupling mediated by band holes in a purely FM semiconductor superlattice.

We now discuss the monotonic ferromagnetic decay of the interlayer exchange within the context of the corresponding phenomenon in metallic multilayers where oscillatory interlayer exchange coupling is commonly observed in well-prepared samples. In that case, the oscillatory dependence of the coupling on spacer thickness is understood using a model that relates the interlayer exchange to spin-dependent reflection at interfaces and resultant quantum-confined states within the spacer.[1] As the spacer-layer thickness is changed, the energy of these quantum-well states changes. The oscillation period is then determined by the filling and emptying of these states as they pass through the Fermi energy of the spacer. The oscillation period is thus directly related to critical spanning vectors of the spacer-layer Fermi surface and in a simple free-electron gas picture is given by $\frac{\pi}{k_F}$. Such a model also predicts that the amplitude of the oscillatory coupling will be damped with an inverse dependence on t_{spacer}. If these concepts are applied to an ideal, disorder-free $Ga_{1-x}Mn_xAs$/GaAs/MnAs trilayer, it is apparent that the oscillation period will be much longer than in a metallic system, simply because of the smaller carrier density in the semiconductor spacer. For instance, for a hole density $p \sim 10^{19}$ cm^{-3}, the Fermi wave vector $k_F \sim 0.67$ nm^{-1} so that the oscillation period is $\sim$5 nm. Thus, even in an ideal sample, we would not expect to observe an oscillatory coupling over the spacer thicknesses studied in our experiments. It is however difficult to ignore the presence of disorder in our samples; the low-temperature growth of the p-GaAs spacer results in a low carrier mobility and a short Drude mean-free path ($\sim$4 nm). Under these circumstances, the smearing of the Fermi surface can rapidly quench the oscillatory Ruderman-Kittel-Kasuya-Yoshida interaction. This could also account for the exponential decay in the amplitude of the coupling rather than the weaker inverse dependence on t_{spacer} expected in the ideal case.

Nonoscillatory FM coupling in multilayers can also arise from extrinsic effects; the most trivial example is that of direct FM coupling through pin holes. This is ruled out by detailed TEM studies of our samples that show that the spacer layer is continuous with no obvious pin holes. Another possible extrinsic effect arises from the interdiffusion of magnetic ions into the nominally nonmagnetic spacer. Experimental studies of Fe/Si/Fe trilayers with a thin ($<$1.6 nm) undoped Si spacer showed exponentially decaying *antiferromagnetic* coupling with both bilinear and biquadratic terms.[19] This AF coupling was interpreted using a model that attributes the coupling to the polarization of paramagnetic loose spins in the spacer layer.[20] The FM nature of the coupling observed in our samples is however contrary to the predictions of this model. In addition, previous studies[21] of Mn interdiffusion in GaAs/MnAs superlattices suggest that the interdiffusion is limited to a several monolayers and is thus not extensive enough to produce the observed effect. Finally, an exponentially decaying exchange coupling was observed in exchange-biased trilayer systems wherein an AFM biasing layer is separated from a FM layer by a noble metallic spacer layer.[22] Again, due to the vast differences in electronic structure and the density of states, it seems unlikely that there would be a common underlying physical mechanism that can describe the exponentially decaying coupling in both our samples and these metallic AFM/noble metal/FM trilayers.

VIII. MODIFICATION OF T_C IN $Ga_{1-x}Mn_xAs$/MnAs HETEROSTRUCTURES

The final section of this paper addresses an intriguing possibility: is it possible that the exchange coupling between

MnAs and $Ga_{1-x}Mn_xAs$ could "bootstrap" the onset of ferromagnetism in the latter via a "proximity" effect? Recent x-ray magnetic circular dichroism studies have suggested that such a proximity effect results in room-temperature ferromagnetism in a very thin region of $Ga_{1-x}Mn_xAs$ within $Fe/Ga_{1-x}Mn_xAs$ bilayers, although no direct evidence for such an effect is observed in magnetometry.[9] The growth of MnAs on top of $Ga_{1-x}Mn_xAs$ consistently enhances T_C of the latter typically by ~25 K compared to single epilayers of $Ga_{1-x}Mn_xAs$ grown under similar conditions [an example is shown in Fig. 4(c)]. The as-grown bilayer samples can show T_C of up to 150 K, much higher than can normally be achieved before annealing. To better understand the nature of this effect and to see if it is intrinsic to the exchange coupling, such bilayer samples were measured after removing the top MnAs with a chemical etch. Figure 4(d) shows the results of this control experiment; the T_C of the $Ga_{1-x}Mn_xAs$ layer remains elevated after etching the sample, instead of dropping as would be expected if the enhancement originated in a proximity effect. Our results thus suggest that the enhancement of T_C is likely an extrinsic effect, stemming from very effective annealing of Mn interstitial defects during the overgrowth of MnAs. To further confirm this hypothesis, the single epilayer control sample was annealed under similar conditions and found to have a very similar increase in T_C [Fig. 4(d)]. We note that our magnetometry measurements cannot of course rule out the existence of exchange-enhanced ferromagnetism in a thin interfacial region of $MnAs/Ga_{1-x}Mn_xAs$ bilayers like what was seen in iron-capped $Ga_{1-x}Mn_xAs$ bilayers.[9]

IX. SUMMARY

In summary, we have reported a comprehensive study of exchange coupling in hybrid FM metal/semiconductor heterostructures. Our study maps out the variation in the interfacial exchange coupling between MnAs and $Ga_{1-x}Mn_xAs$ in bilayers as a function of a variety of system parameters. The resulting data are consistent with the formation of a partial exchange spring configuration in the soft $Ga_{1-x}Mn_xAs$ layer. Studies of trilayer samples show that this exchange coupling can propagate through a *p*-doped nonmagnetic spacer layer, resulting in an interlayer exchange coupling. Using a metallic FM layer to exchange-bias $Ga_{1-x}Mn_xAs$ offers a new test bed for studying exchange coupling between FM metals and semiconductors, and it also possibly provides a model system to study spin-dependent transport in nonuniform magnetization configurations.[23,24] As an engineering tool, it opens up opportunities for tailoring the coercivity of FM semiconductors for proof-of-concept device applications.

ACKNOWLEDGMENTS

This research is supported by the ONR MURI program under Contract No. N0014-06-1-0428. This work was performed in part at the Penn State Nanofabrication Facility, a member of the NSF National Nanofabrication Infrastructure Network. We thank Michael Flatté and Mark Stiles for insightful discussions.

*nsamarth@psu.edu

[1] M. D. Stiles, J. Magn. Magn. Mater. **200**, 322 (1999).
[2] E. Y. Tsymbal and D. G. Pettifor, *Solid State Physics* (Academic, New York, 2001), Vol. 56, pp. 113–237.
[3] D. D. Awschalom and M. E. Flatte, Nat. Phys. **3**, 153 (2007).
[4] B. J. Kirby, J. A. Borchers, X. Liu, Z. Ge, Y. J. Cho, M. Dobrowolska, and J. K. Furdyna, Phys. Rev. B **76**, 205316 (2007).
[5] J. H. Chung, S. J. Chung, S. Lee, B. J. Kirby, J. A. Borchers, Y. J. Cho, X. Liu, and J. K. Furdyna, Phys. Rev. Lett. **101**, 237202 (2008).
[6] K. F. Eid, M. B. Stone, K. C. Ku, O. Maksimov, P. Schiffer, N. Samarth, T. C. Shih, and C. J. Palmstrom, Appl. Phys. Lett. **85**, 1556 (2004).
[7] Z. Ge, W. L. Lim, S. Shen, Y. Y. Zhou, X. Liu, J. K. Furdyna, and M. Dobrowolska, Phys. Rev. B **75**, 014407 (2007).
[8] M. Zhu, M. J. Wilson, B. L. Sheu, P. Mitra, P. Schiffer, and N. Samarth, Appl. Phys. Lett. **91**, 192503 (2007).
[9] F. Maccherozzi, M. Sperl, G. Panaccione, J. Minar, S. Polesya, H. Ebert, U. Wurstbauer, M. Hochstrasser, G. Rossi, G. Woltersdorf, W. Wegscheider, and C. H. Back, Phys. Rev. Lett. **101**, 267201 (2008).
[10] T. Jungwirth, W. A. Atkinson, B. H. Lee, and A. H. MacDonald, Phys. Rev. B **59**, 9818 (1999).
[11] M. Zhu, M. J. Wilson, P. Mitra, P. Schiffer, and N. Samarth, Phys. Rev. B **78**, 195307 (2008).
[12] S. Mack, R. C. Myers, J. T. Heron, A. C. Gossard, and D. D. Awschalom, Appl. Phys. Lett. **92**, 192502 (2008).
[13] D. Mauri, H. C. Siegmann, P. S. Bagus, and E. Kay, J. Appl. Phys. **62**, 3047 (1987).
[14] Z. J. Guo, J. S. Jiang, J. E. Pearson, S. D. Bader, and J. P. Liu, Appl. Phys. Lett. **81**, 2029 (2002).
[15] A. Sugawara, H. Kasai, A. Tonomura, P. D. Brown, R. P. Campion, K. W. Edmonds, B. L. Gallagher, J. Zemen, and T. Jungwirth, Phys. Rev. Lett. **100**, 047202 (2008).
[16] M. Cubukcu, H. J. von Bardeleben, K. Khazen, J. L. Cantin, M. Zhu, M. J. Wilson, P. Schiffer, and N. Samarth, J. Appl. Phys. **105**, 07C506 (2009).
[17] J. Nogues and I. Schuller, J. Magn. Magn. Mater. **192**, 203 (1999).
[18] M. S. Lund, W. A. A. Macedo, K. Liu, J. Nogués, I. K. Schuller, and C. Leighton, Phys. Rev. B **66**, 054422 (2002).
[19] G. J. Strijkers, J. T. Kohlhepp, H. J. M. Swagten, and W. J. M. de Jonge, Phys. Rev. Lett. **84**, 1812 (2000).
[20] J. Slonczewski, J. Appl. Phys. **73**, 5957 (1993).
[21] M. J. Wilson, G. Xiang, B. L. Sheu, P. Schiffer, N. Samarth, S. J. May, and A. Bhattacharya, Appl. Phys. Lett. **93**, 262502 (2008).
[22] N. J. Gökemeijer, T. Ambrose, and C. L. Chien, Phys. Rev. Lett. **79**, 4270 (1997).
[23] J. Foros, A. Brataas, Y. Tserkovnyak, and G. E. W. Bauer, Phys. Rev. B **78**, 140402(R) (2008).
[24] P. M. Levy and S. F. Zhang, Phys. Rev. Lett. **79**, 5110 (1997).